

# Lab on a Chip

Accepted Manuscript



This is an *Accepted Manuscript*, which has been through the Royal Society of Chemistry peer review process and has been accepted for publication.

*Accepted Manuscripts* are published online shortly after acceptance, before technical editing, formatting and proof reading. Using this free service, authors can make their results available to the community, in citable form, before we publish the edited article. We will replace this *Accepted Manuscript* with the edited and formatted *Advance Article* as soon as it is available.

You can find more information about *Accepted Manuscripts* in the [Information for Authors](#).

Please note that technical editing may introduce minor changes to the text and/or graphics, which may alter content. The journal's standard [Terms & Conditions](#) and the [Ethical guidelines](#) still apply. In no event shall the Royal Society of Chemistry be held responsible for any errors or omissions in this *Accepted Manuscript* or any consequences arising from the use of any information it contains.

## Lab on a Chip

### A multi-scale PDMS fabrication strategy to bridge the size mismatch between integrated circuits and microfluidics.

Melaku Muluneh and David Issadore

#### Abstract

In recent years there has been great progress harnessing the small-feature size and programmability of integrated circuits (ICs) for biological applications, by building microfluidics directly on top of ICs. However, a major hurdle to the further development of this technology is the inherent size-mismatch between ICs ( $\sim$  mm) and microfluidic chips ( $\sim$  cm). Increasing the area of the ICs to match the size of the microfluidic chip, as has often been done in previous studies, leads to a waste of valuable space on the IC and an increase in fabrication cost ( $> 100x$ ). To address this challenge, we have developed a three dimensional PDMS chip that better straddles the multiple length scales of hybrid IC / microfluidic chips. This approach allows millimeter-scale ICs, with no post-processing, to be integrated into a centimeter-sized PDMS chip. To fabricate this PDMS chip we use a combination of soft-lithography and laser micromachining. Soft lithography was used to define micrometer-scale fluid channels directly on the surface of the IC, allowing fluid to be controlled with high accuracy and brought into close proximity to sensors for highly sensitive measurements. Laser micromachining was used to create  $\sim 50 \mu\text{m}$  vias to connect these molded PDMS channels to a larger PDMS chip, which can connect multiple ICs and house fluid connections to the outside world. To demonstrate the utility of this approach, we built and demonstrated an in-flow magnetic cytometer that consisted of a  $5 \times 5 \text{ cm}^2$  microfluidic chip that incorporated a commercial  $565 \times 1145 \mu\text{m}^2$  IC with a GMR sensing circuit. We additionally demonstrated the modularity of this approach by building a chip that incorporated two of these GMR chips connected in series.

#### Introduction

Hybrid integrated circuit / microfluidic chips harness the nano-scale feature size, the programmability, and the GHz clock rates of modern semiconductor technology and combine them with the biocompatibility of microfluidics.<sup>1-6</sup> Utilizing this approach, chips have been developed for the programmable dielectric and magnetic control of cells,<sup>7-10</sup> detection of sparse soluble biomarkers,<sup>11-14</sup> and the sensing of rare cells<sup>15-17</sup>. While these chips have performed well in laboratory settings, a major hurdle to their further development is the inherent size mismatch between ICs ( $\sim$ mm) and microfluidic chips ( $\sim$ cm). Millimeter-sized ICs can be built with great functionality, primarily because of the nanoscale-features of modern ICs, which allow for enormously dense circuitry.<sup>18</sup> Increasing the area of an IC to match the size of the microfluidic chip ( $\sim 100x$  increase in area), as has often been done in previous studies(**Fig. 1a**),<sup>9,14,16</sup> leads to a waste of valuable space on the IC, greatly increasing fabrication cost ( $> 100x$ ).

To address this challenge, we have developed a three dimensional PDMS chip that straddles the multiple length scales of hybrid IC / microfluidic chips, allowing millimeter-scale ICs to be integrated into a centimeter-sized PDMS chip.(**Fig. 1b**) To fabricate this chip we used a combination of soft lithography and laser micromachining. In this

technique, a PDMS piece matched in size to the IC was bonded directly to the IC's surface. On this PDMS piece, microfluidic channels were defined using soft lithography, allowing fluid to be delivered to the IC with micrometer-scale resolution. *Vias* ( $\sim 50 \mu\text{m}$  diameter) were laser micromachined into this PDMS piece, and aligned to the microfluidic channels using a masking technique.<sup>19</sup> (**Fig. 1c**) These micrometer-sized *vias* allow multiple fluid inputs and outputs to the microfluidic channels, without consuming the valuable space on the IC that conventional millimeter-sized punched holes would occupy. These *vias* connect the microfluidic channels to a larger PDMS piece, which houses fluid channels and connections to the outside world. (**Fig. 1d**) Deeply engraved ( $h \approx 200 \mu\text{m}$ ) laser-machined channels are utilized to supply each of the molded microfluidic channels. The low hydrodynamic resistance of these channels ensure that each of these microfluidic channels are driven with uniform pressures. The aspect ratio of the PDMS channels in our device were on the order of 1, and as such roof collapse was not an issue.<sup>20</sup> The IC connects electronically to the outside world through a custom flexible printed circuit board upon which it is mounted. Making an analogy to computers, the millimeter-sized hybrid IC / PDMS chips act as the CPUs, housing small feature-sizes and dense functionality, and the larger PDMS piece act as the motherboard, connecting multiple chips and providing access to the outside world.

Our technique affords several key advantages. **1.** Multiple ICs can be integrated into a single PDMS piece, enabling ICs to be used in parallel for increased throughput or in series, enabling various types of ICs for increased functionality. **2.** There is no post-processing or additional lithography on the IC required as has been necessary in previous efforts,<sup>1,2,21,22</sup> allowing the technique to be seamlessly extended to many different types of ICs. **3.** Fluidic channels with micrometer-scale resolution can be defined directly over the IC's surface, enabling accurate micrometer-scale control of fluids directly over micrometer-scale sensors and actuators, offering an improvement over the millimeter-scale "bath-tub" channels used in previous studies.<sup>4-6,23</sup> **4.** The all-PDMS construction of the microfluidics enables inexpensive manufacturing. While combining soft lithography and laser micromachining of PDMS has been reported in the literature,<sup>24</sup> it has not previously been applied to the integration of microfluidics with integrated circuits.

To validate our approach, we have built an in-flow magnetic cytometer consisting of commercial sub mm-sized ICs with an integrated GMR sensing circuit. On top of the IC are microfluidics with flow focusing features to direct cells or beads to the GMR sensors. The hybrid chip is  $5 \times 5 \text{ cm}^2$  and the ICs are  $565 \times 1145 \mu\text{m}^2$  ICs. We demonstrated the functionality of the magnetic cytometer by detecting individual  $8.43 \mu\text{m}$  diameter iron oxide loaded polystyrene beads in-flow. To highlight the capability of integrating multiple ICs into a single PDMS chip, we built a device that included two of these GMR sensing chips connected in series.

## Experimental Design

### Cost vs. size analysis

There is a strong motivation to make ICs as small as possible because the cost of an IC is a function of the area of the die  $A_{IC}$ . The reason for this proportionality is twofold: **1.** Because the cost per wafer is constant, the larger the area of the IC then the fewer ICs

can be made per wafer. **2.** Because defect density across the wafer is constant, the larger the area of the die  $A_{IC}$  the lower its manufacturing yield will be. Due to these factors, the cost of an IC  $\$_{IC}$  scales  $\$_{IC} \propto A_{IC}^\alpha$ , where  $\alpha = 2-3$ .<sup>25</sup>

Microfluidics tend to be much larger than ICs for two main reasons. **1.** The features of microfluidic chips are typically  $>100\times$  larger than that of an IC ( $> 1 \mu\text{m}$ ). **2.** The fluid inputs and outputs to microfluidics are macroscopically machined millimeter-sized pieces, often taking up a significant fraction of the footprint of a microfluidic device. These two factors cause microfluidic chips to be difficult to shrink below  $1 \text{ cm}^2$ .<sup>26</sup>

### Hybrid soft lithography / laser engraved PDMS Fabrication Method

To incorporate millimeter-sized ICs with centimeter-sized microfluidics, our fabrication strategy consisted of integrating three separate pieces of PDMS (**Fig. 2a**): **1.** A millimeter-sized piece of PDMS with soft lithography defined microchannels that were aligned and bonded directly to the IC's surface. Through-holes were laser micromachined into this PDMS piece to connect to fluid channels in the centimeter-sized PDMS piece, **2.** A centimeter-sized PDMS membrane with laser micromachined through-holes that lies between the millimeter-sized and the centimeter-sized PDMS pieces, **3.** A centimeter-sized PDMS piece with laser engraved microchannels that delivers fluid to the millimeter-sized PDMS piece and houses fluidic connections to the outside world. This centimeter-sized PDMS piece was supported at its edges with blocks of PDMS to keep it from bending due to gravity.

Each of the separate pieces of PDMS were bonded together by stamping them into spin-coated uncured PDMS on a Si wafer, aligning the pieces together under a stereoscope with a mask aligner, and baking. (**Fig. 2d,e**) This bonding technique created a robust, leak-proof seal of the microfluidic channels. Using this alignment tool,  $50 \mu\text{m}$  diameter *vias* could be aligned with  $\pm 2 \mu\text{m}$  accuracy. All PDMS pieces were fabricated using poly(dimethylsiloxane -PDMS, KR Anderson Company, sylgard/elastomer kit). The design files are included in supplementary material.

The centimeter-sized PDMS piece was fabricated using direct laser micromachining. First, a 3 mm thick layer of PDMS was poured into a plastic petri dish and baked. This piece was then laser engraved with  $h = 200 \mu\text{m}$  thick channels using raster-based laser patterning (**Fig. 2a**) with an infrared laser micromachining system (VLS3, VersaLaser). To fabricate the PDMS membrane, a  $200 \mu\text{m}$  thick layer of PDMS was spin coated (ws-650mz-23npp, Laurell) on a Silicon wafer. This spin coated layer was then laser cut using vector-based laser patterning to make through holes. (**Fig. 2b**)

To fabricate the molded layer, standard single-layer SU-8 soft lithography (SU-8 2025, MicroChem) with  $h = 30 \mu\text{m}$  thick features was used. On this mold, a  $100 \mu\text{m}$  thick PDMS piece was created. (**Fig. 2c**) We laser micromachine *vias* into this piece that were aligned to the molded microfluidic channels<sup>19</sup>. Because it was not possible to align the laser micromachining tool with sufficient resolution ( $\pm 5 \mu\text{m}$ ) to the fluid channels in the molded PDMS piece, we instead used a sacrificial layer of PDMS as a mask to create these through-holes. To this end, we first defined a  $300 \mu\text{m}$  thick PDMS sacrificial membrane that we aligned with the molded PDMS layer under a stereoscope using a mask aligner. We then laser engraved the through-holes through this mask. Because

the sacrificial mask was thicker than the molded PDMS piece, it was able to protect the molded PDMS from the engraving laser except in the locations where the *vias* were defined. Using this technique, 50  $\mu\text{m}$  diameter holes aligned with  $\pm 5 \mu\text{m}$  accuracy could be reliably created.

The integrated circuit sat on top of a flexible circuit board (fPCB), which provided electrical connections to the outside world. We fabricated the fPCB from Peralux (DuPont), which consists of 25  $\mu\text{m}$  of polyamide and 35  $\mu\text{m}$  of copper. To pattern the electrodes, we printed an etch-barrier using a wax printer (Phaser 8560). The copper was etched using Iron(III) Chloride. Following the etch, the PCB was soaked in acetone for 15 seconds to remove the wax. The copper electrodes were then gold plated (Transene, Immersion CF) to facilitate wire bonding to the IC. The IC was bonded to the PCB using epoxy (Gorilla Glue, Original), wirebonded (Singh Nanocenter, University of Pennsylvania), and the wire bonds were encased in epoxy using a cue tip. The purpose of the epoxy was to mechanically protect the wirebonds during the assembly of the chip with the PDMS microfluidics.

## Results

Flow-Focusing onto the surface of the IC. To demonstrate the utility of building micro-scale fluidics directly on top of the IC, we incorporated hydrodynamic focusing to direct fluid over a GMR sensor. (**Fig. 3a**) Our microfluidic geometry caused the sample (*i.e.* a suspension of cells or beads) to be pushed towards the center of the channel by a co-flow of a sheath fluid. (**Fig. 3b**) Flow focusing has utility for detecting cells in-flow because it can be used to force cells to pass in close proximity of the sensor for maximum sensitivity.<sup>15,16</sup> Additionally, as has been shown in the literature,<sup>15</sup> flow focusing allows physical microchannels to be much larger than the size of the cells, effectively reducing the fluidic resistance and thus the risk of clogging. By changing the ratio of flow rates between the sample  $\phi_{\text{sample}}$  and the sheath flow  $\phi_{\text{sheath}}$ , the amount of focusing could be changed proportionally, as has been previously shown in the literature.<sup>15,16,27</sup> (**Fig. 3c**) Flow was controlled using two syringe pumps (New Era, NE1000) and the flow was visualized by flow-focusing water dyed with rhodamine under an epi-fluorescence microscope (Leica, DM4000B). The devices were shown to be robust for multiple uses, and could be reset for future use by cleaning with isopropyl alcohol followed by placement into a desiccator or sterilized using an autoclave.<sup>28</sup>

In-Flow Magnetic Detection. To demonstrate the utility of incorporating millimeter-sized ICs into a microfluidic chip, we built a magnetic cytometer using a commercial differential giant magnetoresistance (GMR) sensor (NVE - AB001-01). Magnetic detection of cells in-flow has recently been demonstrated as a method to detect extremely sparse tumor cells<sup>15</sup> and pathogens<sup>16</sup> directly in unprocessed clinical samples.

Our magnetic cytometer detects beads by measuring the local change in the magnetic field as each individual bead passed over the sensor. The GMR sensors were arranged in a differential Wheatstone Bridge geometry, and their direction-of-sensitivity was oriented to measure the magnetic field in-plane with the IC. The chip sat in an external **B** field orthogonal to the IC's surface, provided by a permanent magnetic. The microfluidic channels directed each bead over a 59x38  $\mu\text{m}^2$  GMR sensor. As a bead



passed over the GMR sensor, the component of its field in-plane with the IC caused an imbalance in the Wheatstone Bridge that could be measured. (**Fig. 4a**) A 1" diameter, 1/2" thick NdFeB (K&J) magnet and the chip were aligned using a custom machined acrylic piece, made using laser micromachining. The field strength at the location of the sensor was approximately 0.3 T, as measured with a Hall sensor (AlphaLab).

The differential Wheatstone Bridge sensor geometry integrated onto the IC affords high sensitivity, and a tolerance for a common mode in-plane field ( $B_{\text{sat}} = 175$  G) between the sensors. (**Fig. 4b**) This tolerance allowed slight misalignments or inhomogeneities from the permanent magnet to be ignored. To maximize signal to noise, the Wheatstone Bridge circuit was driven with an AC voltage with a frequency of  $f = 1$  KHz. The passing of the bead caused a modulation of the amplitude of the AC voltage  $V_{\text{GMR}}$ . (**Fig. 4b**) The output of the GMR chip was AC coupled to a pre-amplifier (PA) with a gain of 20, and a high-pass frequency of  $f_H = 100$  Hz and a low pass frequency of 3 kHz. (Ithaco) The output of the PA was connected to an analog to digital converter, (National Instruments, NI USB-6009) which digitized the signal at 40 kS/s before sending the signal to a computer over USB for analysis. The signal was demodulated in software (MATLAB), leading to a signal  $V'_{\text{GMR}}$  where peaks corresponding to the passing of beads or cells could be readily distinguished. (**Fig. 4c**)

As a model system for cells, we detected magnetically loaded 8.43  $\mu\text{m}$  diameter polymer beads in-flow. (Spherotech, FCM-8052-2 Fluorescent Yellow Carboxyl Magnetic Particles) As each individual bead passed over the sensor, it lead to a distinct signal in the demodulated output  $V'_{\text{GMR}}$ , allowing the passing of individual beads to be resolved. (**Fig. 4d**) As each bead approached the GMR sensor, its in-plane fields lead to a positive change in the resistance. (**Fig 4e**) When the bead was directly over the sensor there was zero net in-plane field, which lead to a zero in the signal. As the bead was leaving the sensor area, its in-plane field lead to a negative change in the resistance. Thus, each passing bead lead to a distinct signal, a positive and a negative peak. The distance between these peaks enabled the beads velocity to be measured. Some variations in the shape of the signal from the passing beads was observed, which we suspect arose from the moment of the beads being slightly off-axis due to their rolling on the bottom of the channel, as has been reported in previous work.<sup>29</sup>

### Multi-chip integration

To highlight the capability of our technique to incorporate multiple millimeter-scale ICs into PDMS based microfluidics, we integrated two of the GMR sensing chips in series. (**Fig. 5a**) To this end, we created two millimeter-sized IC / PDMS chips and integrated them into a single centimeter-sized PDMS chip. Our microfluidic chip had one sample input. The sample was delivered to the first IC, measured, and the output of the first IC was then the input of the second. Both ICs shared the same source of sheath fluid, provided by a single channel that connected to the ICs in a ladder geometry. The low resistance of the engraved channel enabled the sheath flow to be supplied to each of these chips at the same pressure for uniform operation.<sup>29</sup> The performance of the individual GMR sensing chips were unaffected by the multi-chip integration. Micrographs of this chip show its multiple size-scales, the centimeter-scale engraved

PDMS layer and fPCB (**Fig.5c**), the millimeter-sized ICs (**Fig. 5d**), and the micrometer-sized fluid channels and GMR sensors (**Fig. 5e**).

## Discussion

We have developed a technology to incorporate millimeter-sized ICs into centimeter-sized PDMS microfluidic chips. The key innovation of our technique is the combination of soft lithography and laser micromachining of PDMS to create a simple and cost effective fabrication strategy for hybrid IC / microfluidic chips. The use of soft lithography enabled micrometer-scale fluid channels to be incorporated onto the IC's surface, as opposed to a millimeter-scale "bath-tub" channels used in previous studies.<sup>4,21</sup> These lithographically defined channels allow the position of cells to be controlled with high accuracy and for them to be brought into close proximity to sensors for highly sensitive measurement. The combination of soft lithography with laser micromachining, allowed these millimeter-sized PDMS pieces to be connected to one another with fluid channels and to be supplied with fluid connections to the outside world.

The architecture developed in the paper can be extended to a wide range of applications, for which hybrid IC / microfluidic chips have been previously developed.<sup>2,3</sup> The integration of multiple ICs onto a single chip can enable highly parallelized processing of samples. This functionality would be particularly useful for magnetic cytometry, which has previously been used for the highly sensitive detection of rare cells.<sup>15,16</sup> Because these cytometers must measure cells one at a time, they are ultimately limited by the maximum flow velocity that a cell can be moved through a microfluidic channel. By placing sensors in parallel, the throughput of these cytometers can be scaled linearly with the number of chips. Alternatively, multiple chips with different functionality can be integrated, such as dielectric sensing,<sup>17</sup> heating,<sup>31</sup> magnetic sensing,<sup>14,32</sup> or acoustic sorting<sup>33</sup>. This ability to incorporate multiple ICs, enables monolithic microfluidic platforms that include ICs manufactured with incompatible processes, such as CMOS for dielectric sensors,<sup>17,32</sup> specialized high voltage processes for dielectric control of cells,<sup>23,31</sup> or GaAs for Hall effect sensors<sup>15</sup>. With the rapid development of new capabilities in IC based sensing and in microfluidics, this hybrid IC / microfluidic architecture can help incorporate advances from both fields into commercially practical platforms.

## Acknowledgements

This work was supported by the Department of Bioengineering, University of Pennsylvania, a pilot grant from the University of Pennsylvania Nano/Bio Interface Center, National Science Foundation DMR 08-32802, and a pilot grant from the University of Pennsylvania Center for AIDS Research (AI 045008). We are grateful to DuPont for sending us Pyralux to use in our prototype.

## References

1. H. Lee, Y. Liu, D. Ham, R. M. Westervelt, *Lab Chip*, 2007, 7, 331–337.
2. H. Lee, D. Ham, R. M. Westervelt, *CMOS biotechnology*, Springer, 2007.
3. D. Issadore, R. M. Westervelt, *Point-of-care Diagnostics on a Chip*, Springer, 2013.

4. D. Welch, J. B. Christen, *Journal of Micromechanics and Microengineering*, 2013, 23, 035009.
5. A. Wu, L. Wang, E. Jensen, R. Mathies, B. Boser, *Lab Chip*, 2010, 10, 519–521.
6. A. Uddin, K. Milaninia, C.-H. Chen, L. Theogarajan, *Components, Packaging and Manufacturing Technology, IEEE Transactions on*, 2011, 1, 1996–2004.
7. N. Manaresi, A. Romani, G. Medoro, L. Altomare, A. Leonardi, M. Tartagni, R. Guerrieri, *Solid-State Circuits, IEEE Journal of*, 2003, 38, 2297–2305.
8. M. Jenkner, M. Tartagni, A. Hierlemann, R. Thewes, *Solid-State Circuits, IEEE Journal of*, 2004, 39, 2431–2437.
9. T. P. Hunt, D. Issadore, R. M. Westervelt, *Lab Chip*, 2008, 8, 81.
10. D. Issadore, T. Franke, K. A. Brown, R. M. Westervelt, *Lab Chip*, 2010, 10, 2937.
11. P. M. Levine, P. Gong, R. Levicky, K. L. Shepard, *Solid-State Circuits, IEEE Journal of*, 2008, 43, 1859–1871.
12. M. Barbaro, A. Bonfiglio, L. Raffo, A. Alessandrini, P. Facci, I. BarakBarak, *Electron Device Letters, IEEE*, 2006, 27, 595–597.
13. C. Stagni, C. Guiducci, L. Benini, B. Ricco, S. Carrara, B. Samori, C. Paulus, M. Schienle, M. Augustyniak, R. Thewes, *Solid-State Circuits, IEEE Journal of*, 2006, 41, 2956–2964.
14. R. S. Gaster, D. A. Hall, S. X. Wang, *Lab Chip*, 2011, 11, 950.
15. D. Issadore, J. Chung, H. Shao, M. Liong, A. A. Ghazani, C. M. Castro, R. Weissleder, H. Lee, *Sci Transl Med*, 2012, 4, 141ra92.
16. D. Issadore, H. J. Chung, J. Chung, G. Budin, R. Weissleder, H. Lee, *Adv Healthc Mater*, 2013, 2, 1224.
17. D. K. Wood, S.-H. Oh, S.-H. Lee, H. T. Soh, A. N. Cleland, *Applied Physics Letters*, 2005, 87, 184106.
18. C. A. Mack, *Semiconductor Manufacturing, IEEE Transactions on*, 2011, 24, 202–207.
19. M. Ishizuka, M. Li, X. Liu, *US 20030201578 A1*, 2002.
20. E. Delamarche, *et al. Advanced Materials*, 1997, 9.9, 741-746.
21. T. Datta-Chaudhuri, P. Abshire, and E. Smela, *Lab Chip*, 2014, 14, 1753-1766.
22. Y. Huang, and A. J. Mason, *Lab Chip*, 2013, 13, 3929-3934.
23. D. Issadore, T. Franke, K. A. Brown, T. P. Hunt, R. M. Westervelt, *J Microelectromech Syst*, 2009, 18, 1220-1225.
24. M. Muluneh, D. Issadore, *Lab on a Chip*, 2013, 13, 4750-4754.
25. L. Gwennap, *Microprocessor Report*, 1993, 7, 12–16.
26. C. D. Chin, V. Linder, S. K. Sia, *Lab Chip*, 2012, 12, 2118–2134.



27. P. Gravesen, J. Branebjerg, O. Søndergård Jensen. *Journal of Micromechanics and Microengineering*, 1993, 3.4, 168.
28. A. Mata, A. J. Fleischman, S. Roy, *Biomedical Microdevices*, 2005, 7, 281–293.
29. J. Loureiro, C. Fermon, M. Pannetier-Lecoeur, G. Arrias, R. Ferreira, S. Cardoso, P. P. Freitas, *Magnetics, IEEE Transactions on*, 2009, 45, 4873–4876.
30. M. Muluneh, D. Issadore, *Lab Chip*, 2013, 13, 4750-4754.
31. D. Issadore, K. J. Humphry, K. A. Brown, L. Sandberg, D. A. Weitz, R. M. Westervelt, *Lab Chip*, 2009, 9, 1701-1706.
32. P. Liu, K. Skucha, M. Megens, B. Boser, *Magnetics, IEEE Transactions on*, 2011, 47, 3449–3451.
33. T. Franke, A. R. Abate, D. A. Weitz, A. Wixforth, *Lab Chip*, 2009, 9, 2625–2627.
34. J.-L. Fraikin, T. Teesalu, C. M. McKenney, E. Ruoslahti, A. N. Cleland, *Nature nanotechnology*, 2011, 6, 308–313.

## Figure Captions

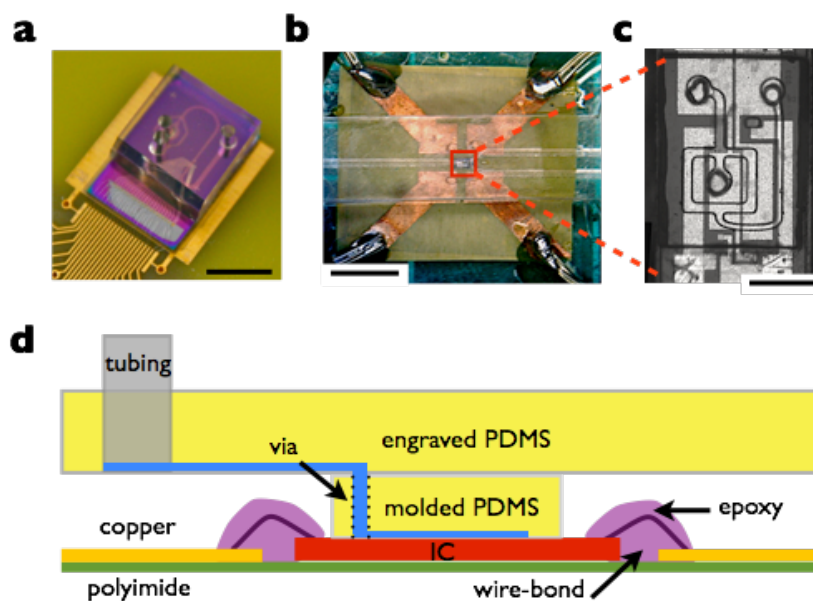


**Figure. 1 Design and implementation of a multi-scale PDMS chip to bridge the size mismatch between integrated circuits (ICs) and microfluidics.** Rather than increase the size of ICs to match the size of microfluidics, as has been done previously (a)<sup>15</sup> we have developed a centimeter-sized PDMS chip (b) that can incorporate millimeter-sized ICs (c). **d.** We combine soft-lithography and laser micromachining to fabricate our chip. A PDMS piece molded by soft lithography sits directly on the IC. Vias 50  $\mu\text{m}$  in diameter were laser machined into this PDMS piece. These *vias* connect to a larger PDMS piece that can connect multiple ICs and houses fluid connections to the outside world. The IC is mounted on a flexible printed circuit board that consists of polyimide and copper. The scale bars are (a) 1 cm (b) 1 cm (c) 400  $\mu\text{m}$ .

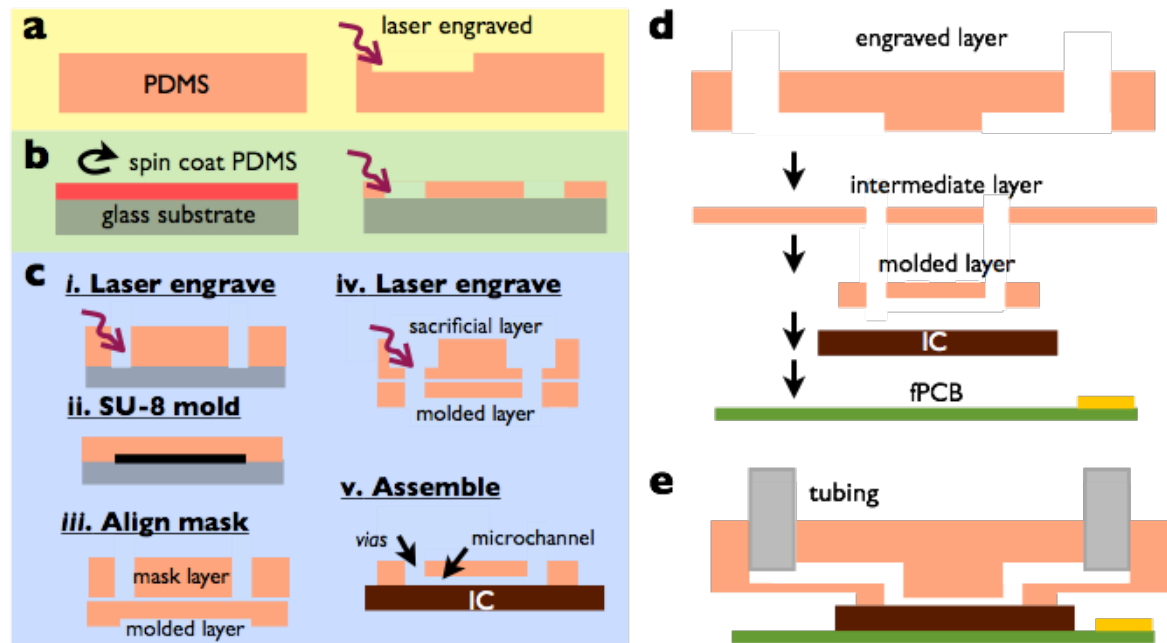


**Figure 2. Hybrid soft lithography / laser micromachined PDMS microchip.** The hybrid chip consists of three PDMS layers, **a**. A laser engraved layer, which includes the delivery microchannels, **b**. a laser cut intermediate layer that contains the through-holes that connect the laser engraved layer and the molded PDMS layer, **c**. a soft lithography molded layer that includes the flow focusing microchannels. The steps to laser micromachine *vias* into the molded PDMS include: i. laser engraving a 300  $\mu\text{m}$  thick PDMS sacrificial layer, ii. SU-8 molding a 100  $\mu\text{m}$  thick PDMS piece, iii. Aligning the sacrificial layer to the PDMS piece, iv. laser engrave the holes through the mask, v. align and bond the PDMS piece to the IC. Uncured and cured PDMS are shown in red and orange respectively. Also shown are the integrated circuit (IC) and the flexible printed circuit board (fPCB). **d**. The layers are aligned and bonded together using a stamping and baking technique, to create the finished 3D micromachined chip (**e**). Illustrations are not drawn to scale.

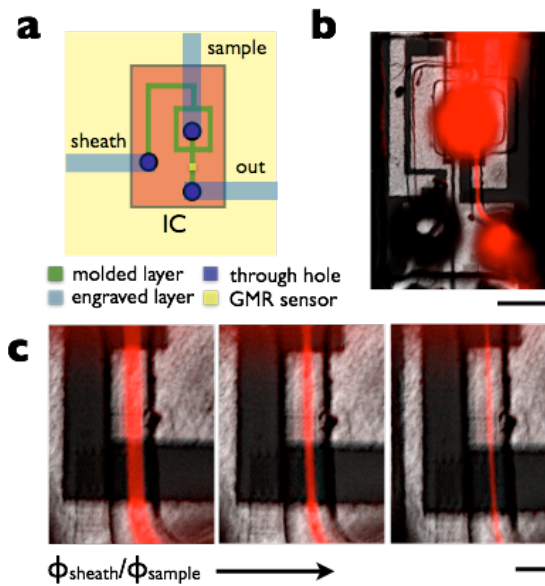


**Figure 3. Hydrodynamic focusing on our hybrid IC / microfluidic chip.** **a.** Flow focusing was implemented to direct fluid over the GMR sensor. **b.** A fluorescence micrograph superimposed on a brightfield image showing flow focusing of water stained with rhodamine on the hybrid chip. The scale bar is  $300 \mu\text{m}$ . **c.** By changing the ratio of the sample and the sheath flow  $\phi_{\text{sample}}/\phi_{\text{sheath}}$  the amount of focusing could be proportionally adjusted. The scale bar is  $30 \mu\text{m}$ .

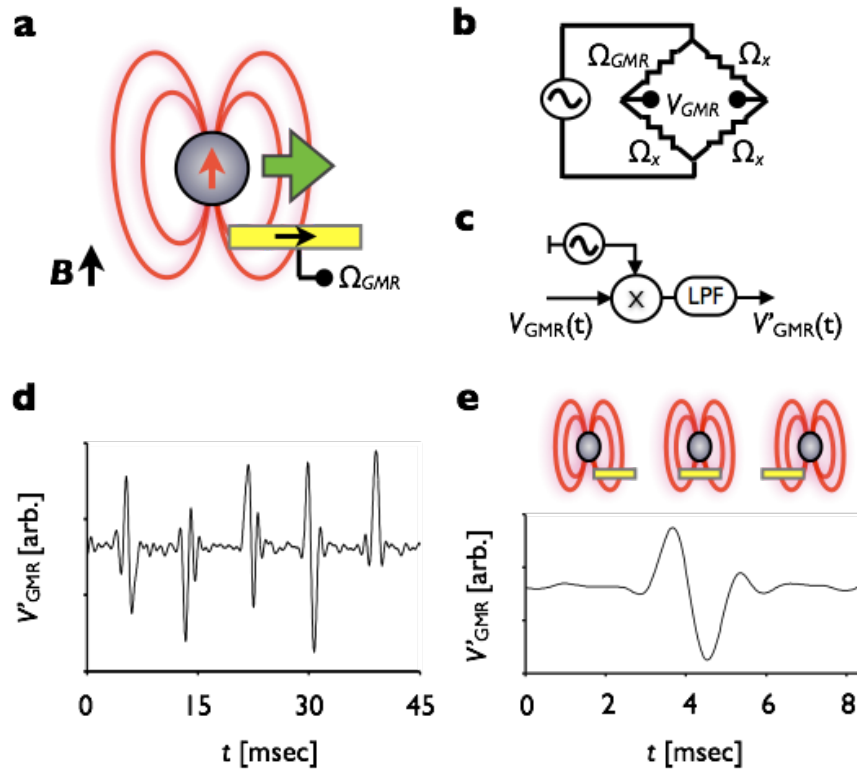


**Figure 4. In-Flow Magnetic Detection.** **a.** As a magnetically labeled bead passed over the GMR sensor, there was a local change in the magnetic field, which resulted in a change in resistance of the sensor  $\Omega_{GMR}$ . **b.** The GMR sensors were arranged in a differential Wheatstone Bridge geometry on the IC. The chip sat in an external  $B$  field orthogonal to the IC's surface, provided by a permanent magnetic. The Wheatstone Bridge circuit was driven with an AC voltage with a frequency of  $f = 1$  KHz. The passing of a bead lead to a modulation of the amplitude of the AC voltage  $V_{GMR}$ . **c.** The signal was demodulated, leading to a signal (**d**) where peaks could be readily distinguished  $V'_{GMR}$ . **e.** As each individual bead passed over the sensor, it lead to a distinct signal in  $V'_{GMR}$ .



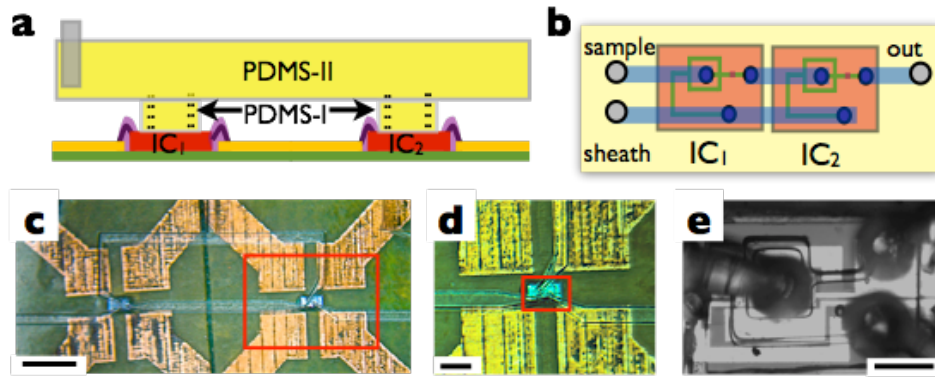


**Figure 5. Multi-chip integration.** **a.** We integrated two GMR sensing chips in series. **b.** Micrographs of this chip show the centimeter-scale engraved PDMS layer and fPCB (**c**), the millimeter-sized ICs (**d**), and the micrometer-sized fluid channels and GMR sensors (**e**). The scale bars are 2 mm, 1 mm, and 500  $\mu\text{m}$  respectively.